

Investigation of thermal and hydrodynamic behaviour of Al₂O₃-water nanofluid through a rough parallel plate

M. Monjurul Ehsan¹, Musfequs Salehin² and A. K. M. S. Islam²

¹Department of Mechanical Engineering, The University of Queensland, Australia.
E-mail: m.ehsan@uqconnect.edu.au

²Department of Mechanical & Chemical Engineering, Islamic University of Technology (IUT), boardbazar, Gazipur-1704, Bangladesh
E-mail: musfequssalehin@iut-dhaka.edu

ABSTRACT

The implementation of nanofluid within a preferred volume fraction in base fluid is one of the innovative and inexpensive methods of enhancing the thermal and hydrodynamic behaviour in terms of increased heat transfer rate and reduced pumping power. In the present paper, forced convection heat transfer and pumping power were studied for a rough parallel plate subjected to constant heat flux under turbulent flow condition. The investigation was performed for a wide range of Reynolds number 10,000 to 30,000 with Al₂O₃ nanoparticles volume fraction 1% to 5% dispersed in base fluid water and three different rough surfaces (relative roughness: 0.001, 0.002, and 0.003) were considered. Heat transfer performance was substantially improved more by employing roughness at the wall of the boundary than the smooth parallel plate and also for the increased more volume fraction of nanofluid than base fluid water. Augmentation was found significant at higher surface roughness and volume fraction by the virtue of superior thermo-physical properties of nanofluid up to 36.9% and 26.1% for the rough surface. Roughness did not increase the pumping power as its effect was mitigated by the nanofluid. 2% volume fraction of Al₂O₃-water nanofluid on 0.003 relative roughness that showed the superior behaviour for heat transfer enhancement with minimum pumping power requirement.

Keywords: Heat transfer improvement; forced convection; nanofluid; surface roughness; pumping power.

INTRODUCTION

Heat transfer in engineering applications has become a major issue for researchers and engineers for the last few decades because of several reasons; among them is the sustainable energy management which demands reduction of the energy loss including the development of more efficient and cost-effective heat exchanger by the implementation of nanofluids as working fluid invested by Hussein et al. [1]. Nanofluids are popular heat transfer fluids made up of a base fluid and nanoparticles. The execution of nanoparticles into heat transfer base fluid significantly enhances the heat transfer performance of the working fluids [2-7]. Solid nanoparticles have a higher thermal conductivity which supports the overall thermal and hydrodynamic properties of the heat transfer fluid as investigated by Li et al. [8] and Cheng et al. [9]. Aly, W. I. [10] investigated laminar flow and heat transfer behaviours of Al₂O₃ (36 nm) and CuO (29 nm), nanofluids flowing through an annular coiled tube heat exchanger with constant

wall temperature boundary condition and found their superiority over the base fluid (water), obtaining maximum enhancements in heat transfer coefficient which were 44.8% and 18.9% for CuO/water and Al₂O₃/water, respectively. The pressure loss was seven times in comparison to water for CuO/water and about two times for Al₂O₃/water nanofluid. Thermal and hydrodynamic performances of a miniature tangential heat sink were investigated experimentally by Miry et al. [11] using Al₂O₃-H₂O and TiO₂-H₂O nanofluids. The effects of flow rate and volume concentration on the thermal performance were investigated for the Reynolds number 210 to 1,100. Experimental results showed that the average convective heat transfer coefficient increased 14 and 11% using Al₂O₃-H₂O and TiO₂-H₂O nanofluid compared to pure distilled water. Thermal and hydrodynamic behaviour in the scraped surface heat exchanger in laminar flow condition was investigated by Ali et al. [12] and significant improvement was obtained in heat transfer coefficient. Combined effects of thermal and concentration jump were analysed in the magneto-hydrodynamic (MHD) flow of nanofluid bounded by a stretching surface by Awais et al. [13]. Das et al. [14] investigated numerically and experimentally how the nanofluid increase the thermal conductivity mixing with base fluid for the better utilisation of heat transfer application as well as several factors affecting thermal conductivity; including types of nanoparticles, solid volume fraction, different base fluids, temperature, particle size, pH, sonication, surfactants, and various mechanisms of thermal conductivity enhancement in nanofluid development discussed. Maximum 16% enhancement in heat transfer by using magnetite nanofluid was obtained by Goharkhah et al. [15]. A hybrid nanoparticle with ethylene glycol (1%-4% volume concentration) was used to measure the thermal behaviour in a double heat exchanger for laminar condition by Hussein et al. [16]. Hydrodynamic and thermal performances for nanofluid was also analysed by Kurian et al. [17] with stainless steel wire mesh blocks by comparing various nanofluids (Al₂O₃, ZrO₂, TiO₂ and SiO₂) with different turbulent models Mahdavi et al. [18]. Thermal and hydrodynamic behaviour on surface roughness was investigated by Mohammadi et al. [19], 21-78% increase in heat transfer using artificially roughened solar air heater by Behura et al. [20], laminar flow heat transfer and pressure drop characteristics in the rough micro channel by Zhang et al. [21].

Heris et al. [22] performed experimentation to observe the enhancement of heat transfer rate for laminar flow using Al₂O₃-water Nanofluid through a circular pipe for a wide range of Peclet number 2,000 to 6,000 and volume fraction of 0.2% to 2.5%. Bianco et al. [23] reported an improvement of a Nusselt number of Al₂O₃-water nanofluid in a circular tube with an increase of Reynolds number and volume fraction adopting both single and multiphase analysis. Laminar flow was considered for a range of Reynolds number 200 to 1200 and volume fraction 1% to 4%. Maiga et al. [24] investigated heat transfer enhancement for forced convection utilising γ - Al₂O₃-water and γ - Al₂O₃-ethylene glycol nanofluids inside a uniformly heated circular tube under constant heat flux for both laminar and turbulent flow conditions. The thermal performance of different types of channels using nanofluid and converting the macrochannel to a parallel arrangement of mini channels for (Re = 125–20000), which improved 70% of the heat transfer enhancement was investigated by Kanikzadeh et al. [25]. Fotukian and Esfahany [26] reported significant improvement of heat transfer and studied the pressure drop of CuO-water nanofluid through a circular tube for a range of Reynolds number of 5,000-33,000. Nasiri et al. [27] found enhancement of heat transfer with Al₂O₃ and TiO₂ nanoparticles dispersed into water through an annular duct under constant wall temperature for a range of Reynolds number 4,000 to 12,000 and volume fraction 0.1% to 1.5%. Heyhat et al. [28] conducted experiments to observe the enhancement of heat

transfer and pressure drop of Al₂O₃-water nanofluid in a circular tube under constant wall temperature for both laminar and turbulent flow condition. Bayat and Nikseresht [29] numerically analysed the thermal performance and pressure drop in a circular tube under constant heat flux using Al₂O₃ nanoparticles dispersed in EG/water mixture with different volume concentrations (1% to 10%) and Reynolds number ranging from 1,500 to 10,000. Haghighi et al. [30] evaluated the cooling performance of three different water-based nanofluids (Al₂O₃, TiO₂, and CeO₂) through a circular tube for laminar forced convection. Turbulent forced convection heat transfer and pressure drop of Al₂O₃-water nanofluid were investigated experimentally through a concentric tube heat exchanger with and without coiled wire tabulators from Re= 4000 to 20000, volume fraction 0.1-1.6%. All results were compared with water, especially the thermal conductivity enhancement by the nanofluids results in heat transfer enhancement. There was no significant effect on pressure drop from volume fraction of 0.8 and 1.6 as stated by Akyurek et al.[31]. Heat transfer enhancement by different fluid domains and nanofluid implementation was also [32-36].

The literature review indicates that most of the articles discussed on the heat transfer augmentation using nanofluid were in different heat transfer applications but the justification of implementing nanofluid was in terms of increased pumping power that has not been studied elaborately. Moreover, all the papers were considered smooth or only rough surface for specific thermal and hydrodynamic behaviour. Thus, the objective of this research work is to investigate about the mixed effect of nanofluid implementation and rough surfaces for heat transfer behaviour and pumping power requirement and also to find the minimum pumping power requirements at enhanced heat transfer rate.

METHODS AND MATERIALS

Governing Equations

The transport equations used in numerical simulations for the two-dimensional analysis of forced convection heat transfer phenomena under turbulent flow condition is given below [37].

Continuity Equation

$$\frac{\partial}{\partial x_i}(\rho u_i) = 0 \quad (1)$$

Momentum Equation

$$\frac{\partial(\rho u_i u_j)}{\partial x_j} = -\frac{\partial p}{\partial x_i} + \frac{\partial}{\partial x_j} \left[\mu \left(\frac{\partial u_i}{\partial x_j} + \frac{\partial u_j}{\partial x_i} \right) \right] + \frac{\partial}{\partial x_j} (-\rho \overline{u'_i u'_j}) \quad (2)$$

Energy Equation

$$\frac{\partial}{\partial x_i} (-\rho u_i T) = \frac{\partial}{\partial x_j} ((\Gamma + \Gamma_t) \frac{\partial T}{\partial x_j}) \quad (3)$$

where Γ is the molecular thermal diffusivity and Γ_t is the turbulent thermal diffusivity which can be expressed as:

$$\Gamma = \frac{\mu}{\rho Pr'}; \Gamma_t = \frac{\mu_t}{\rho Pr'_t}$$

The SST k- ω model has a similar form to the standard k- ω model. The transport equations for the SST k- ω model are as follows:

$$\frac{\partial}{\partial t}(\rho k) + \frac{\partial}{\partial x_i}(\rho k u_i) = \frac{\partial}{\partial x_j} \left(\Gamma_k \frac{\partial k}{\partial x_j} \right) + \bar{G}_k - Y_k + S_k \quad (4)$$

$$\frac{\partial}{\partial t}(\rho \omega) + \frac{\partial}{\partial x_j}(\rho \omega u_j) = \frac{\partial}{\partial x_j} \left(\Gamma_\omega \frac{\partial \omega}{\partial x_j} \right) + G_\omega - Y_\omega + D_\omega + S_\omega \quad (5)$$

In these equations, \bar{G}_k is the generation of turbulent kinetic energy due to mean velocity gradients. G_ω is the generation of ω . Γ_k and Γ_ω represent the effective diffusivity of k and ω , respectively. Y_k and Y_ω represent the dissipation of k and ω due to turbulence only. D_ω is the cross-diffusion term. S_k and S_ω are the user defined source terms.

Thermal and Fluid Dynamic Analysis

The Reynolds number for the flow of nanofluid is expressed as

$$Re = \frac{\rho_{nf} U_{av} D_h}{\mu_{nf}} \quad (6)$$

where ρ_{nf} , U_{av} , and μ_{nf} represents density, average velocity and viscosity of the nanofluid, respectively. If H is the channel height then hydraulic diameter D_h is expressed by $D_h = 2H$. The rate of heat transfer Q_{nf} to channel wall is assumed to be totally dissipated raising its temperature from inlet fluid bulk temperature T_{bi} to exit fluid bulk temperature T_{bo} . Thus,

$$Q_{nf} = \dot{m}_{nf} C_{P_{nf}} (T_{bo} - T_{bi})_{nf} \quad (7)$$

The definition of bulk temperature T_b is given by

$$T_b = \frac{\int_0^{A_c} u T dA_c}{\int_0^{A_c} u dA_c} \quad (8)$$

where A_c is cross-sectional area of parallel plate. The average heat transfer coefficient, h_c is given by

$$h_c = \frac{Q_{nf}}{(\Delta T)} \quad (9)$$

where ΔT , the temperature difference between the wall and fluid is calculated as $\Delta T = T_w - T_b$, where, average wall temperature, $T_w = \frac{1}{\sigma} \int_0^\sigma T_{w,x} dx$

Hence, the expression of average Nusselt number Nu is defined as follows

$$Nu = \frac{h_c D_h}{k_{tnf}} \quad (10)$$

The pumping power per unit length (W) in turbulent flow is [38].

$$W = \frac{\frac{\pi}{4} D_h^2 U_{av} \Delta P}{L} \quad \text{Where pressure drop, } \Delta P = \frac{f L \rho U_{av}^2}{2 D_h}$$

f denotes the friction factor and L is the length of the test section.

Thermo-Physical Properties of Nanofluid

Density

The density of nanofluid considering water as the base fluid is given by the following correlation reported Pak and Cho[39].

$$\rho_{nf} = \rho_p \phi + \rho_{bf}(1 - \phi) \quad (11)$$

Specific Heat

Specific heat of nanofluid is calculated using the following equation by Corcione et al. [40].

$$C_{nf} = (1 - \phi)C_w + \phi C_p \quad (12)$$

Dynamic Viscosity

The dynamic viscosity of nanofluid is given by the following empirical correlation derived by

$$\frac{\mu_{nf}}{\mu_{bf}} = \frac{1}{1 - 34.87 \left(\frac{d_p}{d_{bf}} \right)^{-0.3} \phi^{1.03}}, \text{ Where } d_{bf} = \left[\frac{6M}{N\pi\rho_{fo}} \right]^{1/3}$$

where M is the molecular weight of the base fluid, N is the Avogadro number, and ρ_{fo} is the mass density of the base fluid calculated at temperature $T_o = 293$ K.

Thermal Conductivity

Thermal conductivity of the nanofluid is calculated by the correlation proposed by Ko and Kleinstreuer [41].

$$k_{nf} = \frac{k_{tp} + 2k_{tb} + 2(k_{tp} - k_{tb})\phi}{k_{tp} + 2k_{tb} - (k_{tp} - k_{tb})\phi} k_{tb} + 5 \times 10^5 \beta \phi \rho_p C_p \sqrt{\frac{K_B T}{\rho_p D}} f(T, \phi) \quad (13)$$

where, $f(T, \phi) = (-6.04\phi + 0.4705)T + (1722.3\phi - 134.63)$

Numerical Model

For the numerical investigation of Al₂O₃-water nanofluid through a rough parallel plate, a numerical domain was considered of channel height 3 mm and length 300 mm for both smooth and rough surfaces in turbulent flow condition. The commercial CFD package-ANSYS Fluent 12.0 was employed to solve the governing equations (continuity, momentum and energy) and the turbulent quantities by finite volume method. Axisymmetric analysis was been applied for faster computation.

Boundary Conditions

A constant heat flux of 5000 W/m² was applied at the wall boundary and the fluid was allowed to flow with uniform velocity at the inlet with an assumption that there was no slip condition for both smooth and rough surfaces. The inlet temperature of entering fluid was considered at 300K. For the smooth surface to be made realisable, K-epsilon turbulent model with enhanced wall treatment and SST k- ω turbulent model were selected considering roughness at the wall boundary for single phase analysis with turbulent intensity taken as 5% of the inlet while pressure outlet was considered for capturing near wall boundary layers.

To ensure fully a developed flow, temperature and pressure readings were considered in the region of 275 mm and 290 mm from the inlet of channel to measure the

heat transfer rate and pressure drop. The simulation was performed for a range of Reynolds number of 10,000 to 30,000 with a range of volume fraction of 1% to 5% by changing the value of thermo physical properties (viscosity, density, specific and heat) in the boundary conditions and with three different values of relative roughness, ε/D of 0.001, 0.002, and 0.003.

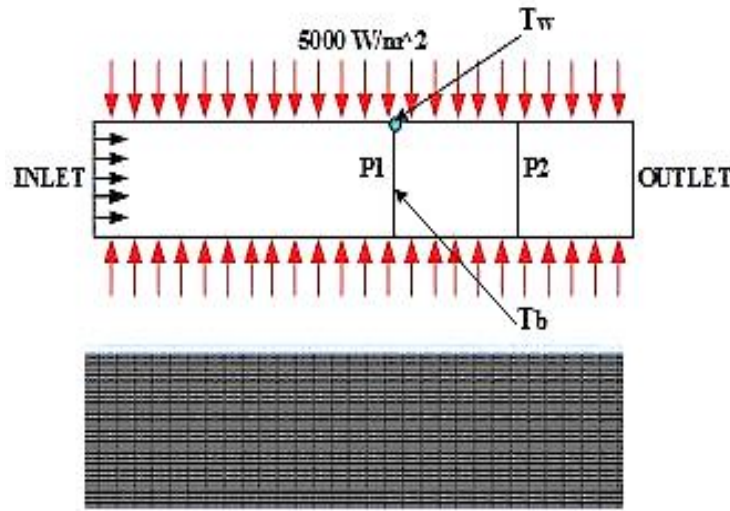


Figure 1. Physical model of the numerical domain and the corresponding mesh.

Grid Independence Test and Code Validation

In order to determine the optimum grid, grid independence test was carried out with water as the working substance flowing through smooth and rough parallel plate with relative roughness $\varepsilon/D=0, 0.001, 0.002$, and 0.003 . Beyond the grid of specific number there was no significant change in Nusselt number. Thus, that is the optimum grid considered for numerical simulation shown in Figure 2. The optimum grid number for plates with relative roughness $\varepsilon/D=0, 0.001, 0.002$, and 0.003 are 36,000; 25000; 45000 and 48,000, respectively.

Code validation was carried out for the validity of numerical results both in smooth and rough surface. For smooth parallel plate calculated Nusselt number was validated with correlation developed by Notter and Sleicher [41], whereas for plates with wall roughness, they were validated with good agreement by the correlation proposed by Prandtl [32] as shown in Figure 2.

The correlation developed by Notter and Sleicher is as follows

$$Nu = 5 + 0.016 Re^a Pr^b \quad (14)$$

$$\text{where, } a = 0.88 - \frac{0.24}{4+Pr} \quad \text{and} \quad b = 0.33 + 0.5e^{-0.6Pr}$$

Prandtl analogy for rough surface is $Nu = St * Pr * Re$

where, Prandtl number is found, $= \frac{\rho * C_p}{K}$; Density (ρ), specific heat of fluid (C_p) and thermal conductivity (K).

$$\text{Stanton Number (St)} = \frac{f}{8} * \left[\frac{1}{1 + 5\sqrt{\frac{f}{8}}(Pr-1)} \right] \quad [15]$$

$$\text{Friction factor, } f = \frac{1.325}{\left[\ln\left(\frac{e}{3.7D} + \frac{5.74}{(Re)^{0.9}}\right) \right]^2}; \text{ for } 5000 \leq Re \leq 10^8, \quad 10^{-6} \leq e/D \leq 10^{-2}$$

where e = Roughness height and D = Channel height, e/D = Relative surface roughness. The present study showed good agreement with those established empirical correlations for rough surface in Figure 2 (for relative roughness 0.003) As well as for smooth plate.

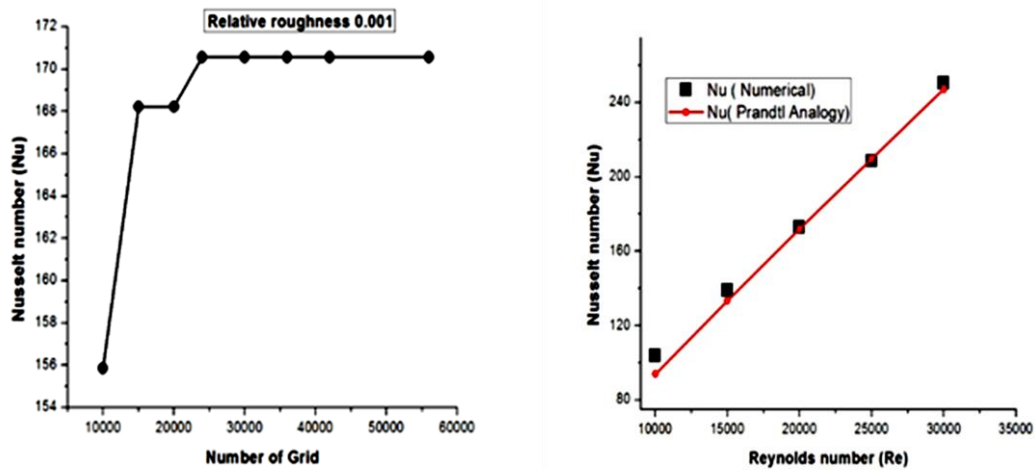


Figure 2. Grid independence study and code validation for rough surface.

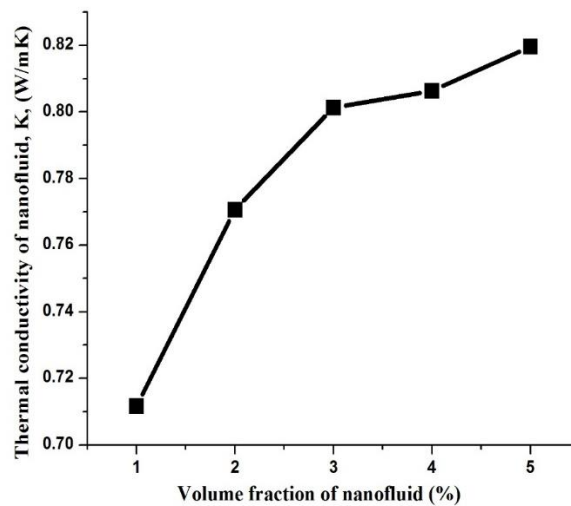


Figure 3. Variation of thermal conductivity of nanofluid with volume fraction.

RESULTS AND DISCUSSION

Effects on Thermophysical and Hydrodynamic Properties

The thermal conductivity, viscosity, density, specific heat, friction factor, and other thermo-physical and hydrodynamic properties were calculated from the established correlations. With increment of volume fraction of nanofluid, the thermal conductivity increases are described in Figure 3. Adversely, the specific heat capacity decreased due

to the increase of volume fraction (Figure 4.) This occurred for the base fluid. Water has the decreasing effect on specific heat capacity mixing with some particular nano particles (Al_2O_3 , CuO etc.[42]. Density also increased in this manner. Hence, it ensures us that the heat transfer rate will be increased with the nanofluid volume fraction as all the thermos-physical behaviours increased. Nanofluid improved amount of viscosity. The viscosity increased with the increase of nanofluid volume fraction (Figure 5.) Viscosity and the surface roughness were the main factors for increasing pumping power.

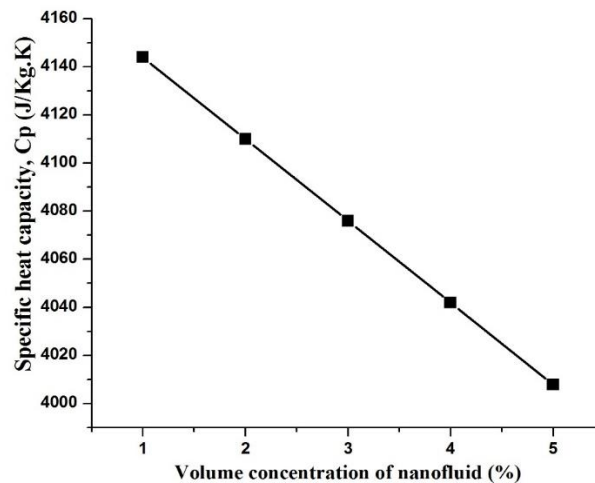


Figure 4. Variation of specific heat capacity due to volume fraction.

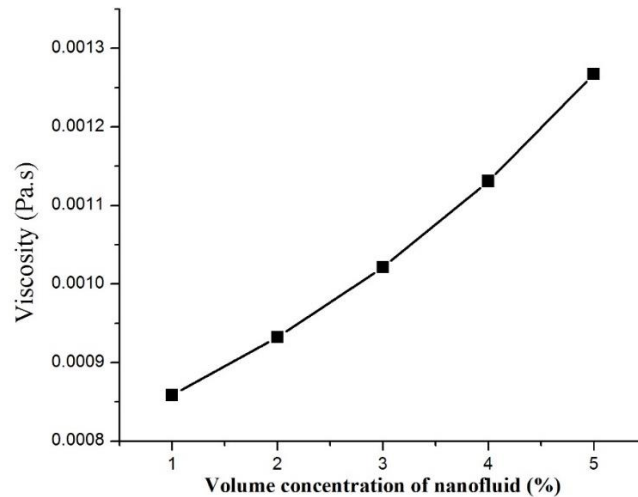


Figure 5. Viscosity due to volume fraction variation.

Figure 6 is plotted based on the characteristic of friction factor with relative surface roughness. For a fixed Reynolds number ($\text{Re} = 20000$) and 2% Al_2O_3 -water nanofluid, friction factor increased with roughness. However, when the roughness was fixed, there was no effect of friction factor on the increasing volume fraction of nanofluid (Figure 7). As the friction factor increased with roughness, the surface roughness was required lower in value to reduce extra pumping power for a specific fluid. On the other hand, there was no increase of friction factor when the nanofluid's volume fraction was

changing. The requirement of pumping power will not be for this reason when the volume fraction of nanofluid varied.

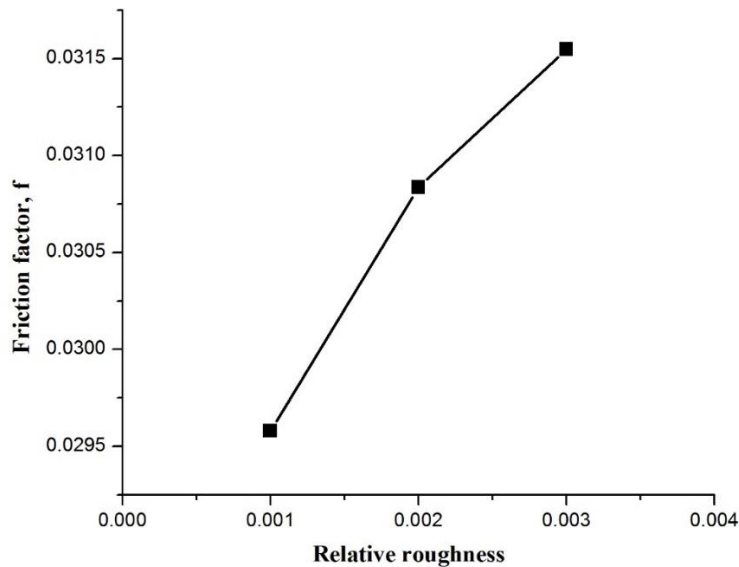


Figure 6. Friction factor due to relative roughness of Re= 20000 and 2% Al₂O₃-water nanofluid.

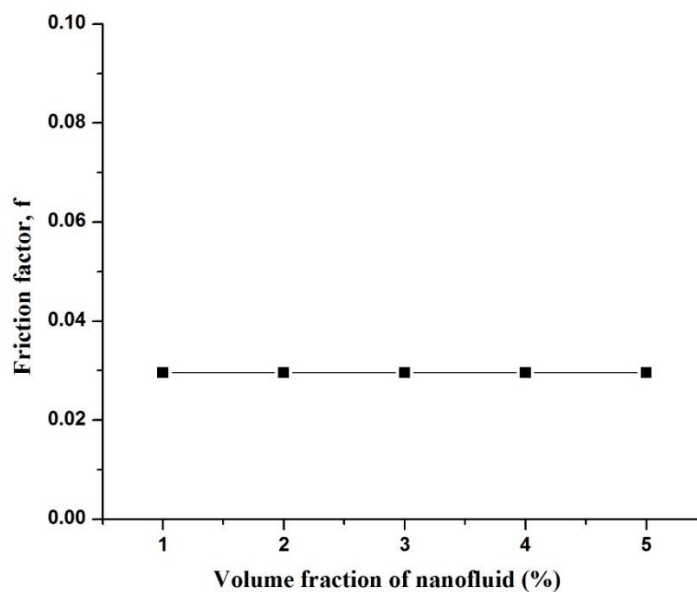


Figure 7. Friction factor due to variation of nanofluid volume fraction for fixed roughness.

Effects of Nanofluid on Heat Transfer and Pumping Power

The superior thermo-physical properties of nanofluid resulted in a significant improvement of convective heat transfer coefficient with an increase of Reynolds number and volume fraction as shown in Figure 8. For Re=25,000, heat transfer coefficient increased by 12.3 % to 36.9% for nanofluid from volume fraction 1% to 5% compared to base fluid water. As water in this study is the base fluid, its availability, inexpensiveness, modified thermal conductivity, good heat transfer rate and optimum viscosity were

compared to other base fluids [43]. The higher improvement of the trend was at the higher Reynolds number. Improvement of the viscosity of nanofluid yields increased pressure head which finally contributed to the higher pumping power requirement [44]. In Figure 9 the pumping power per unit length increased compared to water by 17.5% to 204% for a Reynolds number 30,000.

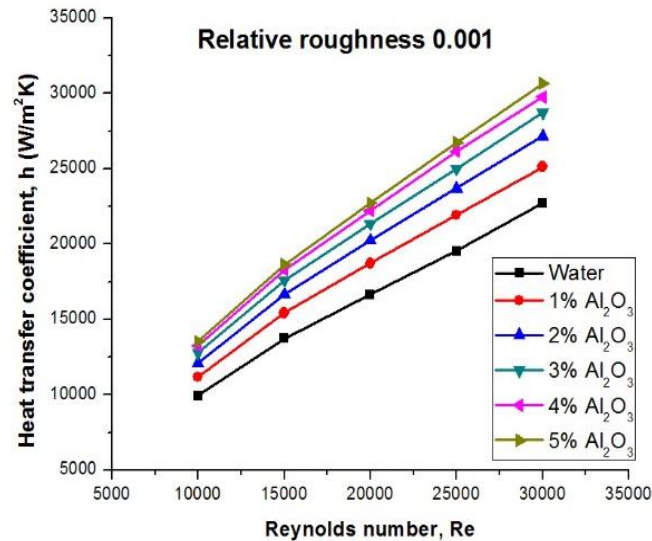


Figure 8. Heat transfer rate augmentation for different volume fractions of nanofluid through a rough surface.

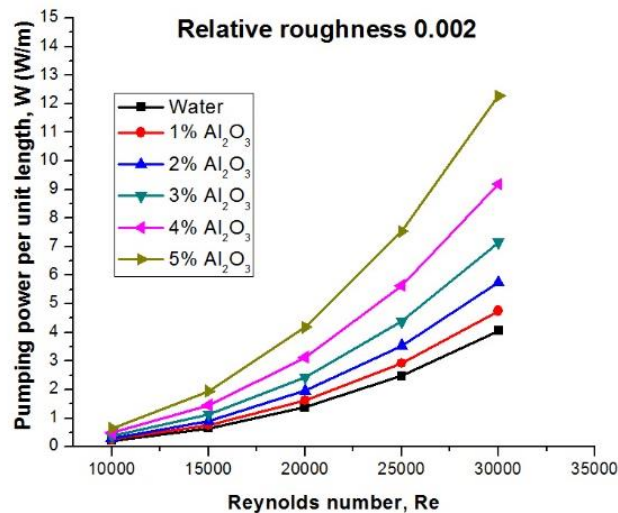


Figure 9. Variation of pumping power requirements for various volume concentrations of nanofluid.

Effect of wall surface roughness on heat transfer and pumping power

Substantial enhancement of heat transfer was observed by introducing wall surface roughness at the boundary of the wall. In Figure 10, the augmentation of convective heat transfer coefficient using rough surface compared to the smooth parallel plate is shown, where the working substance was Al_2O_3 -water nanofluid of volume fraction 3%. By increasing the relative roughness of the wall, $\varepsilon/D=0.001$ to $\varepsilon/D=0.003$, the heat transfer

coefficient increased by 10.9% to 26.1% compared to the smooth plate for Reynolds number of 30,000. Heat transfer enhancement was due to fluid flow on rough surface which happened due to an increase in the surface area and heat transfer coefficient. The change in turbulence pattern for roughness increased the heat transfer coefficient [45]. It was expected to having higher pumping power due to roughness effect because rough surface requires more power for flow but Figure 11 shows exceptional effect. With an increase surface roughness for a fixed volume fraction of nanofluid exhibiting almost the same value of pumping power requirement though nanofluid has higher viscosity. Temperature has an adverse effect on viscosity and for this type of nanofluid, it was investigated by Tang et al. [42] that up to 72% decrease in nanofluid viscosity was by increasing the temperature up to the certain value of nanofluid than water.

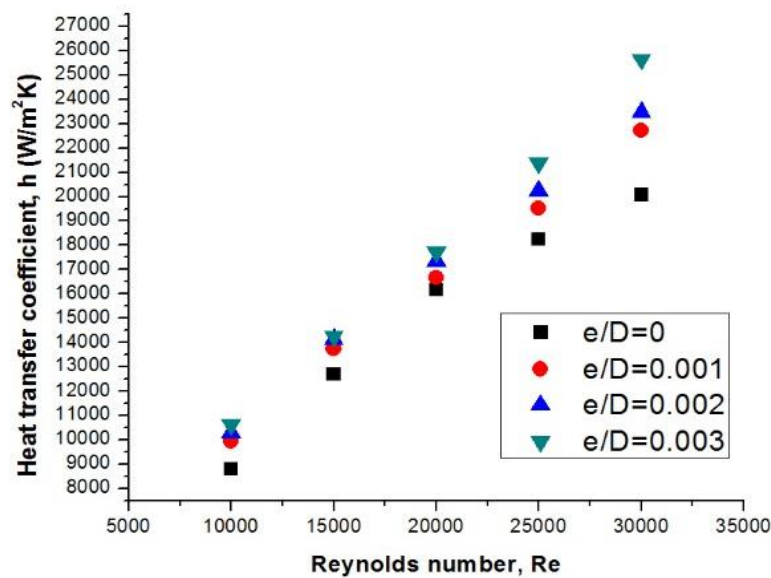


Figure 10. Heat transfer co efficient vs. Reynolds number comparison for nanofluid through different rough surfaces.

Optimum volume fraction in terms of pumping power

The implementation of nanofluid and wall roughness contributed to higher heat transfer coefficient but higher volume concentration of nanofluid had an effect on higher pumping power requirement. As the effect of surface roughness did not make any significant change in pumping power (Figure 11), a change in volume fraction of nanofluid drastically increased the pumping power (Figure 9). On the other hand, if we want more augmentation in heat transfer, then higher volume concentration of nanofluid is required which requires more pumping power. To meet the economic criterion, it is necessary to reduce the pumping power with significant heat transfer enhancement. As the pumping power depends on volume concentration of nanofluid, it is essential to find out the specific volume concentration which requires less pumping power in augmented heat transfer stance.

In Figure 12, the variation of pumping powers with heat transfer coefficient is presented. For finding the minimum pumping power with increased heat transfer rate in the range of $h=22000 \text{ W/m}^2 \text{ K}$ to $34000 \text{ W/m}^2 \text{ K}$ with 0.003 relative roughness was considered. The improvement of reduced pumping power was achieved up to 4% volume fraction of nanofluid and the minimum power of nanofluid was observed 2% of volume fraction. For any value of convective heat transfer coefficient nanofluid with 5% volume

requires more pumping power compared to base fluid water. The optimum volume fractions for rough plates with relative roughness $\varepsilon/D=0.001$ and $\varepsilon/D=0.002$ were found at 3% and 2% of volume concentration, respectively. Due to the higher thermal conductivity of nanofluid than water higher heat transfer rate was achieved at a lower Reynolds number thus minimised the pumping power requirement of nanofluid for a constant heat transfer rate than water.

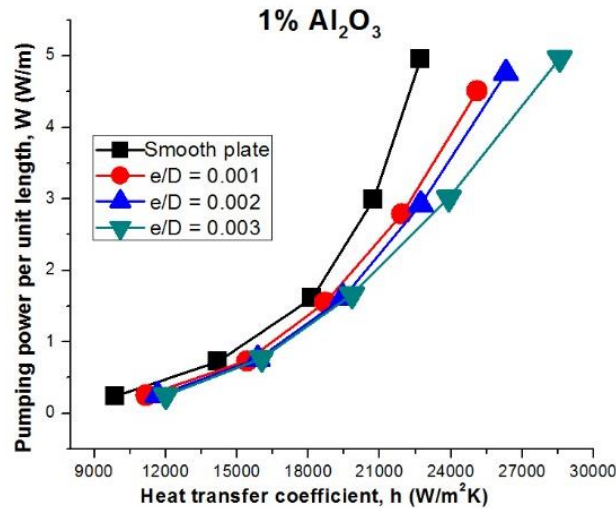


Figure 11. Pumping power requirements by different rough plates.

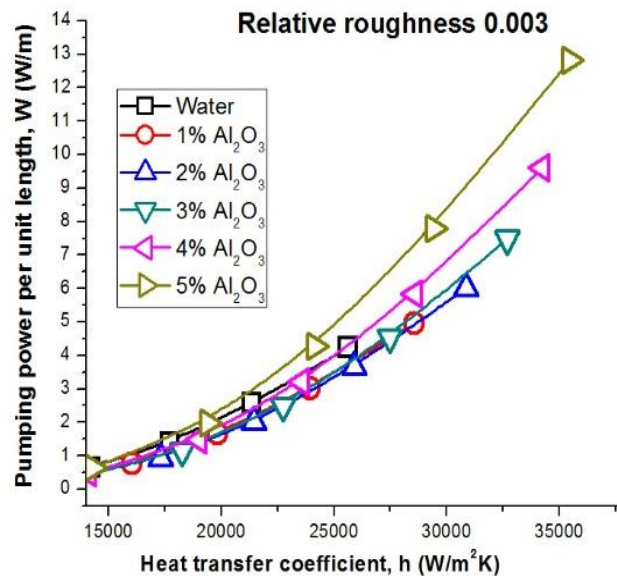


Figure 12. Minimum pumping power requirement for fixed heat transfer rate in the range of $h=22000 \text{ W/m}^2 \text{ K}$ to $34000 \text{ W/m}^2 \text{ K}$.

CONCLUSIONS

In the present paper, the implementation of Al_2O_3 -water nanofluid in rough parallel plates with different relative roughness is investigated. The main objective was to find out the effects and specific volume concentration of nanofluid and specific surface roughness for

obtaining enhanced heat transfer rate which requires less pumping power. We came to some points from the above findings in thermal and hydrodynamic behaviour using nanofluid and surface roughness, which are:

- i) The convective heat transfer rate increased with the increase of nanofluid volume fraction and Reynolds number. Higher volume fraction will give a higher heat transfer rate because of its improved thermal conductivity.
- ii) Heat transfer rate significantly improved with the increasing surface roughness but lower than nanofluid because of a disturbance in the boundary layer.
- iii) The higher volume fraction of nanofluid leads to the requirement of more pumping power in specific surface roughness.
- iv) There was no effect on pumping power with the variation of surface roughness for specific working fluid.

Nanofluid with increased volume fraction can achieve higher heat transfer rate at lower Reynolds number where water or lower volume fraction of nanofluid can achieve that same rate at a higher Reynolds number. More Reynolds number means that extra pumping power is required. As for roughness, the effect on heat transfer was found to have significantly increased but there was no effect on pumping power. Hence, higher roughness and optimum volume fraction of nanofluid can be implemented for enhancing heat transfer rate with minimum pumping power requirement. For this investigation, the performance was better at 0.003 relative roughness with 2% volume fraction of Al₂O₃-water nanofluid.

ACKNOWLEDGEMENTS

Authors are grateful to Mechanical & Chemical Engineering Department, Islamic University of Technology (IUT) for providing computation lab and other facilities.

REFERENCES

- [1] Hussein AM, Bakar R, Kadirgama K. Study of forced convection nanofluid heat transfer in the automotive cooling system. *Case Studies in Thermal Engineering*. 2014;2:50-61.
- [2] Zainal Abidin S, Mohamad S, Bani Hashim AY, Abdullah N, Hafiz MIM, Masripan NAB, et al. Investigation of thermal characteristics of CNF-based nanofluids for electronic cooling applications. *Journal of Mechanical Engineering and Sciences*. 2016;10:2336-49.
- [3] Najiha M, Rahman M, Kadirgama K. Performance of water-based TiO₂ nanofluid during the minimum quantity lubrication machining of aluminium alloy, AA6061-T6. *Journal of Cleaner Production*. 2016;In press.
- [4] Haque ME, Bakar RA, Kadirgama K, Noor MM, Shakaib M. Performance of a domestic refrigerator using nanoparticles-based polyolester oil lubricant. *Journal of Mechanical Engineering and Sciences*. 2016;10:1778-91.
- [5] Zakaria I, Michael Z, Mohamed WANW, Mamat AMI, Azmi WH, Mamat R, et al. A review of nanofluid adoption in polymer electrolyte membrane (PEM) fuel cells as an alternative coolant. *Journal of Mechanical Engineering and Sciences*. 2015;8:1351-66.
- [6] Najiha MS, Rahman MM, Kadirgama K. Parametric optimization of end milling process under minimum quantity lubrication with nanofluid as cutting medium

- using pareto optimality approach. International Journal of Automotive and Mechanical Engineering. 2016;13:3345-60.
- [7] Usri NA, Azmi WH, Mamat R, Abdul Hamid K. Forced convection heat transfer using water- ethylene glycol (60:40) based nanofluids in automotive cooling system. International Journal of Automotive and Mechanical Engineering. 2015;11:2747-55.
- [8] Li CH, Peterson G. Experimental investigation of temperature and volume fraction variations on the effective thermal conductivity of nanoparticle suspensions (nanofluids). Journal of Applied Physics. 2006;99:084314.
- [9] Cheng L, Bandarra F, Enio P, Thome JR. Nanofluid two-phase flow and thermal physics: a new research frontier of nanotechnology and its challenges. Journal of Nanoscience and Nanotechnology. 2008;8:3315-32.
- [10] Aly WI. Thermal and hydrodynamic performance of aqueous CuO and Al₂O₃ nanofluids in an annular coiled tube under constant wall temperature and laminar flow conditions. Journal of Heat Transfer. 2016;138:102401.
- [11] Miry SZ, Roshani M, Hanafizadeh P, Ashjaee M, Amini F. Heat Transfer and Hydrodynamic Performance Analysis of a Miniature Tangential Heat Sink Using Al₂O₃-H₂O and TiO₂-H₂O Nanofluids. Experimental Heat Transfer. 2016;29:536-60.
- [12] Ali S, Baccar M. Numerical study of hydrodynamic and thermal behaviors in a scraped surface heat exchanger with helical ribbons. Applied Thermal Engineering. 2017;111:1069-82.
- [13] Awais M, Hayat T, Ali A, Irum S. Velocity, thermal and concentration slip effects on a magneto-hydrodynamic nanofluid flow. Alexandria Engineering Journal. 2016;55:2107-14.
- [14] Das PK. A review based on the effect and mechanism of thermal conductivity of normal nanofluids and hybrid nanofluids. Journal of Molecular Liquids. 2017.
- [15] Goharkhah M, Ashjaee M, Jamali J. Experimental investigation on heat transfer and hydrodynamic behavior of magnetite nanofluid flow in a channel with recognition of the best models for transport properties. Experimental Thermal and Fluid Science. 2015;68:582-92.
- [16] Hussein AM. Thermal performance and thermal properties of hybrid nanofluid laminar flow in a double pipe heat exchanger. Experimental Thermal and Fluid Science. 2017.
- [17] Kurian R, Balaji C, Venkateshan S. An experimental study on hydrodynamic and thermal performance of stainless steel wire mesh blocks in a vertical channel. Experimental Thermal and Fluid Science. 2017;86:248-56.
- [18] Mahdavi M, Sharifpur M, Meyer JP. Simulation study of convective and hydrodynamic turbulent nanofluids by turbulence models. International Journal of Thermal Sciences. 2016;110:36-51.
- [19] Mohammadi A, Koşar A. Hydrodynamic and Thermal Performance of Microchannels With Different Staggered Arrangements of Cylindrical Micro Pin Fins. Journal of Heat Transfer. 2017;139:062402.
- [20] Behura AK, Prasad B, Prasad L. Heat transfer, friction factor and thermal performance of three sides artificially roughened solar air heaters. Solar Energy. 2016;130:46-59.
- [21] Zhang C, Chen Y, Shi M. Effects of roughness elements on laminar flow and heat transfer in microchannels. Chemical Engineering and Processing: Process Intensification. 2010;49:1188-92.

- [22] Heris SZ, Esfahany MN, Etemad SG. Experimental investigation of convective heat transfer of Al₂O₃/water nanofluid in circular tube. *International Journal of Heat and Fluid Flow*. 2007;28:203-10.
- [23] Bianco V, Chiacchio F, Manca O, Nardini S. Numerical investigation of nanofluids forced convection in circular tubes. *Applied Thermal Engineering*. 2009;29:3632-42.
- [24] Maïga SEB, Nguyen CT, Galanis N, Roy G. Heat transfer behaviours of nanofluids in a uniformly heated tube. *Superlattices and Microstructures*. 2004;35:543-57.
- [25] Kanikzadeh M, Sohankar A. Thermal performance evaluation of the rotating U-shaped micro/mini/macrochannels using water and nanofluids. *Numerical Heat Transfer, Part A: Applications*. 2016;70:650-72.
- [26] Fotukian S, Esfahany MN. Experimental study of turbulent convective heat transfer and pressure drop of dilute CuO/water nanofluid inside a circular tube. *International Communications in Heat and Mass Transfer*. 2010;37:214-9.
- [27] Nasiri M, Etemad SG, Bagheri R. Experimental heat transfer of nanofluid through an annular duct. *International Communications in Heat and Mass Transfer*. 2011;38:958-63.
- [28] Heyhat M, Kowsary F, Rashidi A, Esfehiani SAV, Amrollahi A. Experimental investigation of turbulent flow and convective heat transfer characteristics of alumina water nanofluids in fully developed flow regime. *International Communications in Heat and Mass Transfer*. 2012;39:1272-8.
- [29] Bayat J, Nikseresht AH. Thermal performance and pressure drop analysis of nanofluids in turbulent forced convective flows. *International Journal of Thermal Sciences*. 2012;60:236-43.
- [30] Haghighi EB, Saleemi M, Nikkam N, Anwar Z, Lumbrellas I, Behi M, et al. Cooling performance of nanofluids in a small diameter tube. *Experimental Thermal and Fluid Science*. 2013;49:114-22.
- [31] Akyurek FE, Sahin B, Gelis K, Manay E, Ceylan M. Thermal performance analysis of nanofluids in a concentric heat exchanger equipped with turbulators. *World Academy of Science, Engineering and Technology, International Journal of Mechanical, Aerospace, Industrial, Mechatronic and Manufacturing Engineering*. 2016;10:1517-25.
- [32] Abdolbaqi MK, Azwadi C, Mamat R, Azmi W, Najafi G. Nanofluids heat transfer enhancement through straight channel under turbulent flow. *International Journal of Automotive and Mechanical Engineering*. 2015;11:2294-305.
- [33] Al-Doori W. Enhancement of natural convection heat transfer from the rectangular fins by circular perforations. *International Journal of Automotive and Mechanical Engineering*. 2011;4:428-36.
- [34] Nambeesan KV, Parthiban R, Kumar KR, Athul U, Vivek M, Thirumalini S. Experimental study of heat transfer enhancement in automobile radiator using Al₂O₃/water-ethylene glycol nanofluid coolants. *International Journal of Automotive and Mechanical Engineering*. 2015;12:2857.
- [35] Sundar LS, Sharma K. Laminar convective heat transfer and friction factor of Al₂O₃ nanofluid in circular tube fitted with twisted tape inserts. *International Journal of Automotive and Mechanical Engineering*. 2011;3:265-78.
- [36] Hussein AM, Bakar RA, Kadirgama K, Sharma K. Experimental measurement of nanofluids thermal properties. *International Journal of Automotive and Mechanical Engineering*. 2013;7:850-63.

- [37] A F. 12.0 Theory Guide: Ansys Inc; 2009
- [38] Ozisik MN. Heat transfer: a basic approach. 1985.
- [39] Pak BC, Cho YI. Hydrodynamic and heat transfer study of dispersed fluids with submicron metallic oxide particles. *Experimental Heat Transfer an International Journal*. 1998;11:151-70.
- [40] Corcione M. Heat transfer features of buoyancy-driven nanofluids inside rectangular enclosures differentially heated at the sidewalls. *International Journal of Thermal Sciences*. 2010;49:1536-46.
- [41] Koo J, Kleinstreuer C. A new thermal conductivity model for nanofluids. *Journal of Nanoparticle Research*. 2004;6:577-88.
- [42] Tang CC, Tiwari S, Cox MW. Viscosity and friction factor of aluminum oxide–water nanofluid flow in circular tubes. *Journal of Nanotechnology in Engineering and Medicine*. 2013;4:021004.
- [43] Chein R, Chuang J. Experimental microchannel heat sink performance studies using nanofluids. *International Journal of Thermal Sciences*. 2007;46:57-66.
- [44] Savage D, Myers J. The effect of artificial surface roughness on heat and momentum transfer. *AIChE journal*. 1963;9:694-702.
- [45] Riazi H, Murphy T, Webber GB, Atkin R, Tehrani SSM, Taylor RA. Specific heat control of nanofluids: A critical review. *International Journal of Thermal Sciences*. 2016;107:25-38.